

Diameter and Aggregation Controlled Preparation by Solvothermal Synthesis of Ultra-small Particles CuFe₂O₄

Zihan Huang¹, Siyi Li², He Ding², Piao Pingyang*², Jun Xinhuang¹

1. College of Material Science and Chemical Engineering, Harbin Engineering University (HEU), Harbin 150001, China

2. Institute of Inorganic Nonmetallic Matter (IINM), HEU

Date of first draft: 14/May/2021

Abstract:

Copper ferrite nanoparticles have catalytic activity for hydrogen peroxide, which can be used in many fields. This characteristic comes from the physical properties of matters at nanometer scale. Thus, controlling the size and aggregation of nanoparticles during the synthesis is one of the ways to obtain target performance. In this article, a kind of ultra-small nano particle CuFe₂O₄ with uniform morphology was prepared by solvothermal synthesis. The effects of solvent, reactant molar ratio, reaction temperature, surfactant and reaction time on the yield of CuFe₂O₄, size and morphology of nano particles were investigated under different synthesis conditions. XRD, TEM, EDS were used to analysis the materials, and the physical properties of the products were analyzed. An optimized solvothermal synthesis scheme was proposed.

Key words: Copper Ferrite; Solvothermal Synthesis; Ultra-small Particles; Preparation Control

After the discovery of Fe₃O₄ catalysis, the catalytic performance of some other spinel metal oxides has been paid attention to. MnFe₂O₄ nanoparticles prepared by high temperature pyrolysis have the ability to catalyze the decomposition of H₂O₂ [1]. Some evidences show that CoFe₂O₄, MgFe₂O₄ and other nanoparticles have similar properties [2][3]. Some other crystalline substances also have the ability to catalyze the decomposition of peroxides, by grinding NiFe₂O₄ nanoparticles and H₂O₂ liquid at room temperature, it can result in the decomposition of H₂O₂ [4]. Most transition metal oxides can promote the decomposition of peroxides. For an example, CuO nanosheets with a particle size of 50-80 nm were prepared by the sol gel method, which can catalyze the decomposition of H₂O₂ in PBS solution at 37 °C [5]. NiO nanoparticles were also found to be able to catalyze the decomposition of benzoyl peroxide [6].

When these substances lose the nanometer scale and lose the nanometer effect, the catalytic effect will be greatly weakened [7]. Peroxides often participate in biochemical reactions in cells, so catalase like nanoparticles may play an important role in the field of biomedicine. Thus, it is important to control the diameter of nano particles to gain the expected properties in applications.

1 Principle and Influence Factors

1.1 Catalytic Principle of Iron Based Nanoparticles

Fe₃O₄ nanoparticles were first found to have peroxidase (POD) activity, and the catalytic reaction mechanism is consistent with Fenton reaction mechanism [8]. The conversion between Fe²⁺/Fe³⁺ in a large number of iron atoms on the surface is the key to ensure the catalytic activity of iron based nano particles. H₂O₂ reacts with Fe³⁺ to generate hydroxyl radical, which indicates that Fenton mechanism is consistent with the simulated activity of peroxidase. Under neutral (pH=7.4) and alkaline conditions, no hydroxyl radical was detected

Source: 2021-May IINM Projects

Zihan H., Bachelor, Material Science, HEU

Siyi L., PhD, IINM, HEU

He Ding., Associate Professor, IINM, HEU

Piao P. Yang., Professor, IINM, HEU

Jun X. Huang. Bachelor, Material Science, HEU

by ESR technology, but gas was produced in the reaction, indicating that the mechanism was different from the catalytic activity of POD [9]. In a neutral or alkaline environment, FeOOH^{2+} and hydrogen peroxide radical (HO^{2-}) are generated rapidly and excessively by the combination of Fe^{3+} and H_2O_2 , and then the superoxide anion (O^{2-}) is rapidly ionized from HO^{2-} , and the generated $\text{HO}^{2-}/\text{O}^{2-}$ is further converted into H_2O and O_2 through the reaction with hydroxyl radical, which shows significant hydrogen peroxide catalytic activity [10].

1.2 Catalytic Principle of Ferrite

The test results of atomic absorption spectrometry show that a small amount of iron ions may be leached by Fe_3O_4 magnetic nanoparticles, and the number of ions is too low to show obvious catalytic activity, which further confirms that the activity of iron based nanoparticles mainly comes from iron oxide nanoparticles, rather than leached ions. EPR analysis and free radical inhibition experiment clarified the reaction mechanism based on ferric oxide catalytic degradation of organic pollutants, and the research results showed that $\text{O}^{2-}/\text{HO}^{2-}$ [11] played a dominant role.

1.3 Factors Influence Catalytic Activity of Ferrite

The environment affect the activity of iron based nanoparticles, such as pH and temperature. In addition, the catalytic activity of iron based nanoparticles can also be modified by adjusting the size, morphology of surface and structure. Generally, the larger the size is, the higher the activity is. This is because larger nanoparticles have higher surface area and volume. In the research on Fe_3O_4 , the structure and morphology have an impact on its peroxidase mimic activity. Compared with octahedron, spherical particles have the highest activity because of their high specific surface area [12]. For triangular plates and octahedrons, although they have similar size and surface area, the arrangement of surface atoms leads to differences in activity.

Ferrite nanoparticles can convert the adsorbed hydrogen peroxide molecules into active oxygen such

as hydroxyl radicals and singlet oxygen through the surface oxygen vacancy activation mechanism, but the catalytic efficiency is relatively low. Increasing particle size is a method to improve catalytic efficiency. Because the larger the size of the nanoparticles, the smaller the surface defects, and the fewer the surface bonding ligands, which also reduces the concentration of surface active oxygen vacancies.

The catalytic efficiency can also be improved by optimizing the type and concentration of doped ions. The crystal structure can change the catalytic ability of Fe_3O_4 [13]. Adding metal elements to the matrix will change the crystal field structure of the matter [14]. According to the selection rule of quantum mechanics, the electric dipoles of the 4f electron layer of some ions do not allow interaction. However, by changing the structure of the crystal field, the band gap can be broken, thus increasing the rate that surface defects can catalyze.

2 Research Method

2.1 Preparation Methods

In this research, copper (Cu) was chosen as the doped element. As a transition metal element, copper has many unique properties. In spinel ferrite, which is generally written as formula AFe_2O_4 , the addition of copper can significantly improve the efficiency of catalytic hydrogen peroxide decomposition. Thus, the goal product of synthesis reaction is CuFe_2O_4 . In this experiment, CuFe_2O_4 was prepared by solvothermal synthesis, high temperature pyrolysis of reactants. Different reactions conditions were set to study their influence on diameter of nano particles.

Solvothermal synthesis is similar to the hydrothermal synthesis, but the difference is that the solvothermal synthesis needs to be carried out in a closed container, and the reaction temperature is relatively high, usually between 160 °C and 200 °C [15]. The composition of solvothermal synthesis is mainly divided into four parts: precursor, reductant, dispersant and reaction assistant. By adjusting the reaction conditions (reaction time, reaction temperature) and experimental parameters

(concentration and ratio of reactants, properties of reactants), the morphology and size of crystals can be controlled more accurately. In the preparation process, the factors that can affect the particle size and appearance of the generated particles are the type, amount, reaction time and system of reductant, iron source, dispersant and reaction assistant.

2.2 Analysis Methods

X-ray diffraction (XRD). Cu-K is used in the test α Radiation/graphite monochromator, $\lambda = 0.15405$ nm, scanning speed $15^\circ/\text{min}$; Transmitting current: 200 mA, accelerating voltage: 40 kV, scanning range: 2θ . Generally $10\sim 80^\circ$. The XRD test results were compared with the sample standard diffraction card (JCPDS) (MDI-Jade 5.0 Software) to analyze the crystal phase and composition of the sample. The scanning range is $10^\circ - 80^\circ$.

Transmission electron microscope (TEM). Test voltage: 3.7 kV, acceleration voltage: 200 kV. The morphology, size, structure, dispersion and load information of the tested materials were obtained by low and high power transmission. The type and distribution information of elements in materials were obtained through mapping.

Energy dispersive X-ray spectroscopy (EDS). EDS is used in the test to qualitatively analyze the composition and relative content of elements in the sample test selection area. The preparation process of EDS test sample is to disperse the sample by solvent ultrasonic, then drop it onto the silicon wafer, or directly smear the powder sample on the conductive adhesive. All instruments used in this research were listed in Table.1.

2.3 Variations Control

The variations will base on the composition of solvothermal synthesis, to study the probable influence of solvents molecules and temperature on diameter of nano particles, focusing on the thermal motion of molecules, influence of crystal growth, finally by comparing with the results of others, to provide a practicable synthesis scheme to control scale of nano particles and give explanation.

3 Experiments and Analysis

3.1 Preparation Steps

Take a 100mL three neck flask and put a magnetic rotor inside. Measure 30 mL of solvent, weigh copper acetylacetonate and iron acetylacetonate, weigh the surfactant, and add them to the flask. Shake the flask with ultrasonic for 1 min. Place the flask on the magnetic heating stirrer, connect the condenser tube and temperature sensor, and vacuum. Start heating and stirring, set the stirring to gear 4. Heat to 110°C in sections at 30°C , 50°C and 80°C for 0.5 h at 110°C . Close the vacuum pump, slowly inject nitrogen, set the reaction temperature, and continuously stir for reaction.

Stop heating, cool naturally after the reaction, transfer the substances in the flask to two 50 mL tubes at 60°C . The above experimental steps are carried out in the ventilate cabinet. Add 30 mL absolute ethanol into each of the two branches, centrifuge at 6000 rpm for 10 min. Pour out the supernatant. Dissolve the precipitate in 45 mL absolute ethanol, centrifuge at 6000 rpm for 10 min, and repeat. Dissolve the precipitate in 45 mL ethyl acetate, centrifuge at 6000 rpm for 10 min. Put the tube into a vacuum drying oven, set temperature as 60°C , keep vacuum, and the drying time is 6 h. The diagram of instruments was shown in Fig.1.

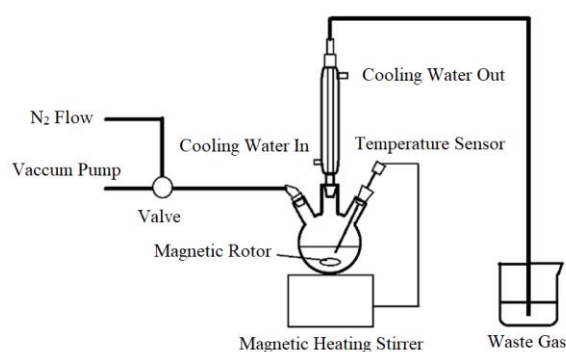


Fig.1 Diagram of Instruments of Preparation Reaction

The first preparation was carried out at 280°C for 0.5 h by using triethylene glycol as solvent [16], but it was found that the prepared product was agglomerated and the particle size was smaller than expected under TEM.

Table.1 List of Instruments

Instrument	Model	Manufacturer
Electronic balance	FA1004	Shanghai Shunyu Hengping Scientific Instrument Co., Ltd
Digital temperature magnetic stirrer	SZCL-2	Gongyi Yuhua Instrument Co., Ltd
Ultrasonic cleaner	KQ-250	Kunshan Ultrasonic Instrument Co., Ltd
Centrifuge	TDL-5A	Shanghai Experimental Instrument Co., Ltd
Electric blast drying oven	101A-1E	Shanghai Fu Experimental Instrument Factory Co., Ltd
Multi-platform magnetic stirrer	JH-6	Jiangsu Jintan Zhongda Instrument Factory
Pharmacist balance	HC.TP11B.5	Beijing Medical Balance Factory
Liquid nitrogen container		Chart Biomedical (Chengdu) Co., Ltd
Vacuum pump	RS-2	Shanghai Shuli Instrument Co., Ltd
pH meter	FE20	Mettler Toledo Instruments (Shanghai) Co., Ltd
X-ray diffractometer	D/MAX- III	Rigaku, Japan
Transmission electron microscope	H-600	Hitachi, Japan
X-ray energy dispersive spectrometer	JXA-840	JEOL, Japan

Table.2 List of Reagent

Reagent	Chemical formula	Purity	Manufacturer
Cupric chloride	CuCl ₂	99.99%	Sinopharm Chemical Reagent Co., Ltd
Ferric chloride	FeCl ₃	99.99%	Sinopharm Chemical Reagent Co., Ltd
Copper acetylacetonate	Cu(acac) ₂	99.99%	Sinopharm Chemical Reagent Co., Ltd
Iron acetylacetonate	Fe(acac) ₃	99.7%	Tianjin Kemio Chemical Reagent Co., Ltd
Sodium hydroxide	NaOH	99.7%	Tianjin Kemio Chemical Reagent Co., Ltd
Oleic acid	C ₁₈ H ₃₄ O ₂	99.7%	Sinopharm Chemical Reagent Co., Ltd
1-Octadecene	C ₁₈ H ₃₆	99.7%	Sinopharm Chemical Reagent Co., Ltd
Cyclohexane	C ₆ H ₁₂	99.7%	Tianjin Fuyu Fine Chemicals Co., Ltd
Absolute ethanol	CH ₃ CH ₂ OH	99.7%	Tianjin Fuyu Fine Chemicals Co., Ltd
Ammonia solution	NH ₃ ·H ₂ O	99.7%	Beijing Chemical Factory Beihua Fine Chemicals Co., Ltd

As long chain molecular solvent can promote the formation and growth of crystal nucleus [17]. In order to explore the influence of solvent molecular weight and molecular chain length on the growth of product particle size, and determine the solvent for subsequent preparation, five different solvents were designed.

First, the inert solvent oleic acid with long chain and large molecular weight was selected to weaken the interference of solvent movement on crystal nucleus growth through its high viscosity. In consideration of the boiling point, the molecular weight and molecular chain length are reduced in turn, and triethylene glycol and glycerol are selected as the solvent without changing the functional group of the alcohol. At the same time, dibenzyl ether, a stable organic solvent, was also selected as an experimental solvent.

The addition of surfactant can significantly affect the morphology and particle size of nanoparticles [18]. In order to explore the influence of different kinds of surfactants and their dosage on particle size of product, three different surfactants were introduced, each corresponding to three doses. They are oleic acid, polyvinylpyrrolidone (PVP) and PEG2000 (Polyethylene glycol). Oleic acid can be used as a surfactant because its long molecular chain and carboxyl end group can form an amphiphilic structure. The methylene group of PVP is a non-polar group, which is lipophilic. Its strong polar bond lactam is hydrophilic and can also act as a surfactant. PEG2000 is often used as surfactant due to the same reason. The doses were set after calculation.

During the reaction, there occasionally remained a purplish red precipitate at the bottom of flask that is

insoluble in concentrated hydrochloric acid at room temperature, but soluble in concentrated nitric acid and generates brownish yellow gas. It can be determined that its composition is copper. To protect copper ions from reduction, and to explore the impact of different feed ratios on product synthesis, three different ratios of reactants were designed through calculation.

Reaction temperature and time can significantly affect the morphology and particle size of nanoparticles [19]. In order to explore the influence of reaction temperature and time on the product synthesis, two reaction temperatures and times were designed. The information of reagents were listed in Table.2. In total, 19 groups of experiments in Table.3 were conducted.

3.2 Products Purification

The preparation results were shown in Table.4. Some precipitates left in the flask are brownish. Based on the previous acid dropping test, it can be judged that all the brownish precipitates are non-ideal synthesis schemes containing simple copper. Thus, these schemes are eliminated.

The precipitation of some schemes after the first centrifugation are high non uniform. The centrifugation product formed two layers along the radial direction of the tube. The color of two layers is visible different to the naked eye. The outer layer is brown or red with metallic luster, and the inner layer is black. This indicates that two substances or two phases are formed. However, copper ferrite of any phase is black and has no metallic luster. Based on the previous experimental phenomena, it can be analyzed that a part of copper was dispersed in the solution. Under strong white light, the products of some schemes are dark brown, indicating that there are still some copper impurities. Table.5 is statistics of products.

After the first centrifugation, no supernatant was obtained in any scheme, indicating that the prepared nanoparticles had good dispersion in ethanol organic solvent, which may be caused by the following two reasons: 1) the interaction between copper ferrite molecule and ethanol leads to special solubility in

ethanol; 2) the nano particles prepared are small in size, they can be well suspended in the solution and maintain stability.

It can be seen from the precipitation stratification that the copper will precipitate first in centrifugation and accumulate in the outer layer of tube. To separate the product from the upper liquid and separate impurities, subsequent centrifugation is performed.

In addition, the dispersity of the precipitate obtained in ethyl acetate is not good, and even if ultrasonic uniformly, the precipitate will occur again after standing for 1h. Considering that some impurities are more soluble in anhydrous ethanol, in order to separate the main product, the following steps were carried out: the upper liquid obtained after the first centrifugation was mixed with anhydrous ethanol ethyl acetate of different proportions and centrifuged at 12000 rpm for 10 minutes. The purpose of adding ethyl acetate is to reduce the percentage of ethanol in the solution. First, it can make the copper ferrite dissolved in ethanol enter the supersaturated state and precipitate. Second, if ethanol interacts with copper ferrite, the addition of ethyl acetate can reduce the solubility of copper ferrite in ethanol. The designed volume ratio of ethanol to ethyl acetate and the obtained results are shown in Table.6.

Table.6 Ethanol: ethyl acetate volume ratio & centrifuge results

Ratio	Precipitate	Color	Supernate
1:0	Few	Black	Turbid Black
1:2	Less	Black	Turbid Black
1:3	Huge	Black	Clear yellow
1:4	Huge	Black	Clear yellow

Samples without ethyl acetate still has only few precipitation at the 12000 rpm centrifugation, while the samples with ethyl acetate has huge precipitation, which can obtain clear yellow supernatant. The yellow supernatant needs to be washed again. Separate the precipitate, and repeat the above centrifugation to obtain colorless and clear supernatant. The ethanol/ethyl acetate volume ratio of 1:3 was selected to blend with the upper liquid of other schemes, and the purified samples of each scheme were obtained after centrifugation at 12000 rpm for 10 min twice.

Table.3 Nineteen Groups of Preparation Schemes

No.	Cu: Fe Mole ratio	Solvent	Surfactant	Dosage	Reaction Tem(°C)	Reaction Time(h)
A10011	1:2	Triethylene glycol			280	0.5
B10011	1:2	Oleic acid			280	0.5
C10011	1:2	Tetraethylene glycol			280	0.5
D10011	1:2	Glycerol			280	0.5
E10011	1:2	Benzyl ether			280	0.5
A12111	1:2	Triethylene glycol	Oleic acid	1mL	280	0.5
A12211	1:2	Triethylene glycol	Oleic acid	2mL	280	0.5
A12311	1:2	Triethylene glycol	Oleic acid	4mL	280	0.5
A13111	1:2	Triethylene glycol	PVP	0.2g	280	0.5
A13211	1:2	Triethylene glycol	PVP	0.5g	280	0.5
A13311	1:2	Triethylene glycol	PVP	1.0g	280	0.5
A14111	1:2	Triethylene glycol	PEG2000	0.2g	280	0.5
A14211	1:2	Triethylene glycol	PEG2000	0.5g	280	0.5
A14311	1:2	Triethylene glycol	PEG2000	1.0g	280	0.5
A10021	1:2	Triethylene glycol			210	0.5
A10012	1:2	Triethylene glycol			280	1.0
A10022	1:2	Triethylene glycol			210	1.0
A20011	2:4	Triethylene glycol			280	0.5
A30011	1:3	Triethylene glycol			280	0.5

Table.4 Results of Preparation Schemes

No.	Reactants solution	After reaction	Bubble	Precipitate	Color	1 st centrifugation precipitate
A10011	Reddish brown	Black	Medium	Less	Black	Less
B10011	Tawny	Reddish brown	Less	Huge	Purplish brown	Huge
C10011	Reddish brown	Black	Huge	Medium	Black	Huge
D10011	Reddish brown	Black	Medium	Medium	Black	Medium
E10011	Reddish brown	Black	Medium	Medium	Black	Medium
A12111	Reddish brown	Black	Less	Medium	Black	Medium
A12211	Reddish brown	Black	Less	Medium	Black	Medium
A12311	Reddish brown	Brown	Less	Huge	Brown	Huge
A13111	Reddish brown	Black	Medium	Medium	Black	Medium
A13211	Reddish brown	Black	Medium	Less	Black	Medium
A13311	Reddish brown	Black	Medium	Less	Black	Less
A14111	Reddish brown	Black	Less	Medium	Black	Medium
A14211	Reddish brown	Black	Less	Less	Black	Less
A14311	Reddish brown	Black	Less	Less	Black	Less
A10021	Reddish brown	Black	Less	Less	Black	Less
A10012	Reddish brown	Black	Less	Medium	Black	Huge
A10022	Reddish brown	Black	Less	Less	Black	Less
A20011	Reddish brown	Black	Less	Less	Black	Huge
A30011	Yellowish brown	Black	Less	Medium	Black	Medium

Table.5 Statistics of Centrifugation Product Status

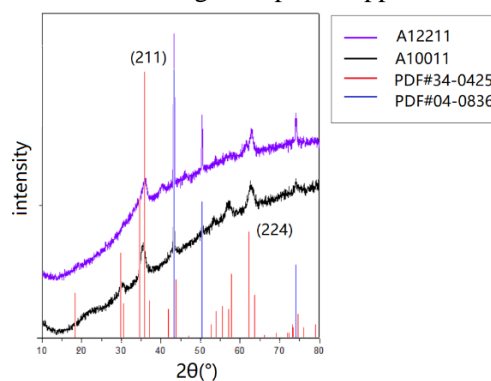
No.	Layered (Y/N)	Color of precipitate	Color under strong light	Color of upper liquid
A10011	N	Black	Black	Black
C10011	Y	Brown/black	Brown	Black
D10011	Y	Brown/black	Brown	Black
E10011	N	Black	Dark brown	Black
A12111	N	Black	Dark brown	Black
A12211	Y	Brown/black	Brown	Black
A13111	N	Black	Black	Black
A13211	N	Black	Black	Black
A13311	N	Black	Dark brown	Black
A14111	N	Black	Black	Black
A14211	N	Black	Black	Black
A14311	N	Black	Black	Black
A10021	N	Black	Black	Black
A10012	N	Black	Black	Black
A10022	N	Black	Black	Black
A20011	N	Black	Black	Black
A30011	N	Black	Black	Black

3.3 XRD Test and Analysis

The samples of several representative schemes are tested by X-ray diffraction. Because the surfactant mainly affects the morphology and particle size of the product, the process of its combination with nanoparticles occurs after the nanoparticles grow to a certain size. Therefore, when it is added in a small amount as a surfactant, its influence on the lattice is not considered. In the scheme using oleic acid as solvent, the black product was not obtained and the product was insoluble in concentrated hydrochloric acid at room temperature, so the XRD test was not carried out on this scheme. The test of the scheme using triethylene glycol as solvent and oleic acid as surfactant was planned, because the scheme using oleic acid as solvent cannot synthesize the target product, so it is necessary to confirm whether the product contains copper ferrite in this scheme. A total of seven schemes, A10011, C10011, D10011, E10011, A12211, A20011 and A30011 were tested by XRD.

For A10011 and A12211, triethylene glycol is used as the solvent, and other synthesis conditions are the same.

After 2mL oleic acid is added as the surfactant, it is obvious that in the XRD spectrum, Fig.2, 2θ at 43.0° , 50.5° and 74.0° , sharp and obvious peaks (PDF#04-0836) belong to copper simple substance, which indicates that the addition of oleic acid directly leads to the formation of copper simple substance, which is also consistent with the phenomenon that there is no target product in the solution using oleic acid as solvent, but a large amount of copper simple substance is generated. The characteristic peaks of tetragonal spinel copper ferrite (PDF#34-0425) [20] appeared at 35.8° and 62.1° of A10011 and A12211, respectively corresponding to the (211) and (224) crystal planes of tetragonal spinel, indicating that the products synthesized by these two schemes contain tetragonal spinel copper ferrite.

**Fig.2** XRD spectrogram of A10011 and A12211

For A20011 and A30011 in Fig.3, when 2θ at 43.0° and 50.5° , peaks belong to copper is obviously occur (PDF#04-0836). There are peaks at 35.8° and 62.1° that conform to the characteristics of tetragonal spinel copper ferrite (PDF#34-0425), corresponding to (211) and (224) crystal planes of tetragonal spinel respectively, indicating that the products of these two schemes contain copper ferrite. However, the content of copper in these two schemes is too high.

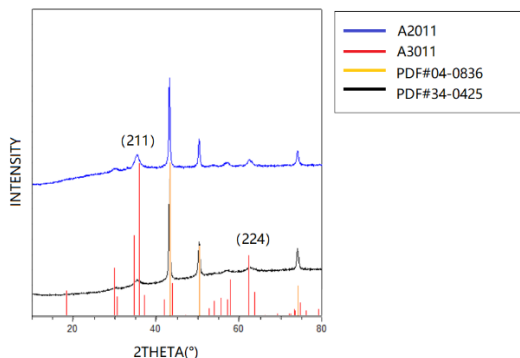


Fig.3 XRD spectrogram of A20011 and A30011

In Fig.4, for C10011 and E10011, there are peaks at 35.8° and 62.1° with the characteristics of tetragonal spinel copper ferrite (PDF#34-0425), which correspond to (211) and (224) crystal planes of tetragonal spinel respectively, indicating that the products of these two schemes contain copper ferrite. For C1011, there is an obvious peak belonging to copper at 43.0° (PDF#04-0836). D10011 has only the bulge of silicon dioxide substrate, without any other crystal phase peak.

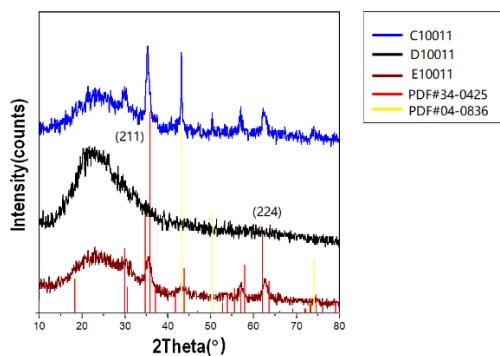


Fig.4 XRD spectrogram of C10011, D10011 and E10011

3.4 TEM Test and Analysis

As the schemes with oleic acid and glycerol as the

solvent does not synthesize the target product, and the scheme with oleic acid as the surfactant contains too much copper simple substance, the samples in the above schemes will not take TEM test. In addition, when the amount of PVP and PEG2000 additives is 1.0g, the products that can be separated are extremely limited, the samples of these two schemes are not able to take TEM test. The factors that affect the morphology of nanoparticles are reaction temperature, time and chemical environment (solvent, surfactant), and the molar ratio of the reactants mainly affects the crystal form of the product [21]. Therefore, TEM test is not conducted for the schemes to change the reactants ratio. For the scheme with synthesis temperature of 210°C , TEM test could not be taken because too few products were obtained after washing. Thus, TEM test were taken on the samples of 8 schemes (Fig.5), A10011, C10011, E10011, A13111, A13211, A14111, A14211 and A10012.

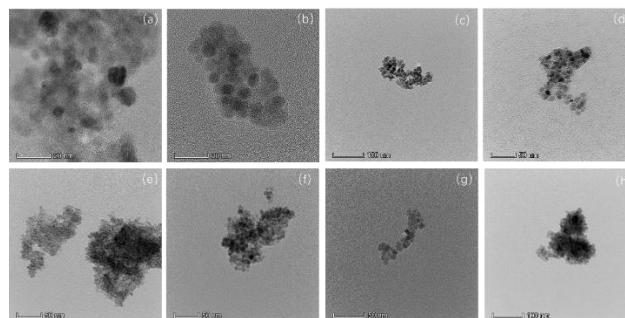


Fig.5 TEM Photos. A10011(a), C10011(b), E10011(c), A13111(d), A13211(e), A14111(f), A14211(g), A10012(h).

Calculate particle size by Digital Micrograph (Table.7). Take the horizontal and vertical centerline of the aggregate, divide into four parts, randomly select five particles that the boundary can be distinguished clearly.

Table.7 Statistic of Particles Size and Aggregation

No.	Average size(nm)	Variance	Aggregation
A10011	9.8	20.8	Medium
C10011	8.9	6.7	Medium
E10011	9.9	10.8	Light
A13111	9.7	18.7	Light
A13211	5.8	12.6	Strong
A14111	8.8	15.4	Strong
A14211	9.6	9.2	Light
A10012	9.8	14.9	Strong

The size of nanoparticles obtained in the above eight schemes is in the range of 8-12 nm, with little difference. However, there are obvious differences in particle size uniformity and morphology regularity among different schemes.

In A10011, the particles are continuously distributed, and a single particle is in an irregular spherical or amorphous state. The particle size of larger particles is 3-5 times that of smaller particles, which is not uniform enough. In C10011, the particles are island shaped, the width of the island is 20-40 nm, the length width ratio of the island is about 3:1, the morphology of a single particle is relatively regular spherical, and there is no significant difference in particle size. The statistical variance is small, which indicates that the particle size is uniform. In E1001, the particles are distributed as island, the width of the island is 50-80 nm, and the length is 150-200 nm. The island is further composed of islands with a width of 20-40 nm and a length of 40-50 nm. The combination area between the islands can be clearly observed. The shape of a single particle is relatively regular, basically spherical, and the particle size is relatively uniform, but it is not as ideal as C10011. The particles in A13111 are island shaped. Most of the islands are 50-80 nm width and about 100 nm length. They are also composed of islands. The island diameter is about 20 nm. The area of each island can be clearly identified. The morphology of individual particles is sphere, rectangular and other shapes, which are nonuniform, and the particle size difference is also large.

In A13211, the particles are island distributed, the diameter of the island is 50-100 nm, and the island is a continuous phase. The island substructure cannot be distinguished, but the size of its single particle is smaller than other schemes, which is between 5-8 nm, the particles are nearly spherical, with little difference in particle size. In A14111, the particles are island shaped, with a diameter of 80-120 nm, and consists of small islands with a diameter of about 50 nm. The shapes of single particles are mainly rectangular and circular, with nonuniform morphology and large difference in particle size. In A14211, the particles are distributed in a long strip shape, with a length of about 100 nm and a width of 20-50 nm. A few of the single

particles are spherical and most of them are irregular in shape, but the size is relatively uniform. This might be the deformation of the product due to its light agglomeration, more particles directly acting on the surface and higher exposed surface area. It may also be the deformation caused by PEG2000 binding on the product surface. In A10012, the particles are island phase dispersed, with a diameter of 150-200nm. It can be observed that the island is composed of secondary structures with a diameter of 80-100nm. The shape of a single particle is approximately circular, and the particle size is relatively uniform.

As the reaction temperature approaches the boiling point of solvent, the vibration of solvent molecules plays an important role in the synthesis of nano materials, especially ultra-small nanoparticles [22].

Table.8 shows the boiling point at one atmospheric pressure, relative molecular weight and the ratio of reaction temperature to boiling point R_b of the three solvents. At the reaction temperature, triethylene glycol is closer to the boiling point than tetraethylene glycol, which means that there are more superheat zones in the triethylene glycol solvent. In the superheat zone, molecules change from liquid to gas to generate bubbles, which is an extremely unstable process, generating more shocks and vibrations. This action on the nano particles will result in irregular morphology of the products.

Table.8 Parameters of Three Solvents

Solvent	Molar mass	Boiling point	R_b (%)
Tetraethylene glycol	194.23g/mol	327.3°C	83.96
Triethylene glycol	150.17g/mol	288.0°C	94.92
Benzyl ether	198.26g/mol	298.0°C	95.24

From tetraethylene glycol to triethylene glycol and then to dibenzyl ether, the molecular length of solvent is decreasing. Fig.6 shows the molecular structure of the three solvents. For molecules with the same functional group type, the longer the molecular chain, the weaker the vibration at the same temperature [23]. Therefore, the interference of triethylene glycol molecules on the formation of products at 280°C is more serious than that of tetraethylene glycol, which shows larger particle size distribution and more irregular morphology in the TEM

photos. However, the molecule of dibenzyl ether is a shorter chain, and the space that can be affected is limited when the molecular motion and conformational transformation occur. In addition, the molecule of dibenzyl ether has no terminal hydroxyl, so its affinity for copper ferrite nanoparticles is not as strong as alcohol. On the contrary, the π bond of benzene ring has a high electron density [24], which can repel the lone pair electrons on the surface of copper ferrite. This explains why the products synthesized with tetraethylene glycol as solvent have better morphology and particle size uniformity than those of triethylene glycol system. However, dibenzyl ether has little effect on the morphology and particle size of the product near the boiling point due to its small molecule and difficulty in binding to copper ferrite.

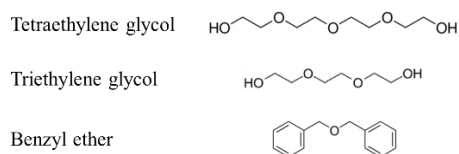


Fig.6 Molecular Structure Formula of the Solvents

Aggregation in each scheme is obviously different (Fig.5). It can be judged from Fig.5(a) and Fig.5(d) that the addition of PVP reduces the number of amorphous particles and improves the shape regularity of nanoparticles. PVP is bound to the particle surface after the particles grow to an extent, and its polymer chains protect the particles from the impact of solution molecules, playing a certain buffer role, but at the same time, they hinder the migration of ions from the liquid phase to the solid phase, limiting the growth of crystals. When the surface of nanoparticles binds PVP molecules to an extent (not necessarily saturated), its size cannot continue to increase. Therefore, when the dose of PVP increases, it can be observed from the TEM that the size of a single particle decreases instead (Fig.5(d) and Fig.5(e)).

However, the addition of PVP did not significantly alleviate the aggregation of nano particles (Fig.5(a) and Fig.5(d)), because the aggregation and growth of nanoparticles are simultaneous processes. For the initially formed crystal nucleus, PVP is a polymer with high molecular weight, large moment of inertia, and PVP terminal groups do not have strong polar groups.

The newly formed nanoparticles have light mass, small volume, and small surface area, It is not enough to bind PVP molecules by surface adsorption. The process of PVP binding nano particles occurs after the nanoparticles grow to a certain size, so the aggregation of particles is not significantly alleviated. However, it can be observed from Fig.5(d) and Fig.5(e) that with the increase of the dosage of PVP added, the aggregation of the obtained products even increases, which may be caused by the following reasons.

The molecular backbone of PVP is a carbon chain structure, which is highly soluble in alcohols. One end of PVP is adsorbed on the surface of nano particles, and the other end is affinity for triethylene glycol molecules. The adsorbed end directly conducts the tension from the solution. Under the effect of the tension, the space surrounded by PVP has a tendency to merge, as shown in Fig.7. This trend is related to the dosage of the surfactant. When the concentration of the surfactant is higher, the molecules bound to the nanoparticles are more (under the unsaturated state of the particle binding site), and the surface tension of the transferred solvent is greater, the particles are easier to merge, with a trend of reducing system energy.

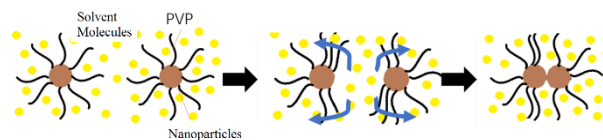


Fig.7 Diagram of PVP Promoting Aggregation

In addition, this is also related to the strength of the binding between surfactant and nanoparticles. The weaker the binding strength, the more conducive to the merger. The binding between PVP and the surface of nanoparticles is mainly electrostatic adsorption, and the binding strength is weak. With the addition of larger dose of PVP, the degree of aggregation of products increases, which can be explained. Besides, the appearance of island structure can also be explained. Under the aggregation of PVP, the particles first form a secondary structure, and then aggregate again to form a large island structure, which was seen by TEM.

In the scheme using PEG2000 as the surfactant, it can be observed that the addition of PEG2000 improves the uniformity of the product particle size and morpho-

logical regularity (Fig.5(a), Fig.5(f)). The addition dose of PEG2000 has little effect on the product particle size (Fig.5(f), Fig.5(g)), It is speculated that the added PEG2000 has not yet saturated the binding of nanoparticles. The effect of PEG2000 on aggregation is opposite to that of PVP. With the increase of PEG2000 dosage, the aggregation of the product is significantly reduced, which is due to the combination of PEG end groups and the surface of the nanoparticles, which is a stronger combination to disperse the island structure of the nanoparticles. When the reaction time is extended to 1h, TEM photo (Fig.5(h)) shows that the product is obviously in a serious aggregated state. However, the particle size does not change notably, which indicates that the nucleation process occurs first. With the extension of the reaction time, the main process is that the initial crystal nuclei gradually gather to form a larger cluster structure.

3.5 EDS Test and Analysis

From the above results, A14211 was considered as the best of 19 schemes. The product of A14211 was tested by EDS, and the element type distribution in the nanoparticles was obtained (Fig.8).

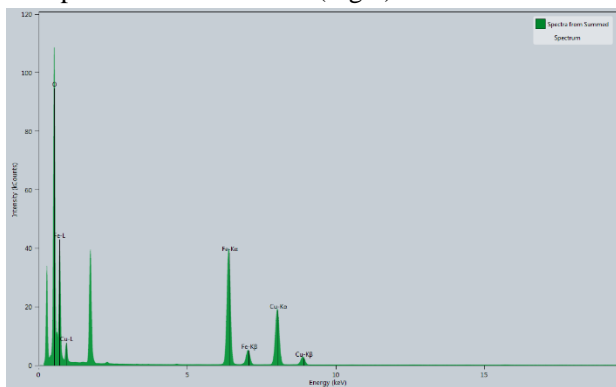


Fig.8 EDS Spectrum of A14211 Product

The peak value of oxygen element was the highest. By solving the peak integral intensity, the oxygen content was approximately twice as much as iron and 4 times as much as copper, which was in agreement with the molar ratio of the target product CuFe_2O_4 . But iron has Fe-K α and Fe-K β two peaks, copper element has Cu-K α and Cu-K β two peaks, both are K α mainly. During the formation of copper ferrite crystal, spinel and anti-spinel crystal structures are both formed, that is, due to

the difference of local ion concentration and driving force during the formation of a small number of products, the positions occupied by iron atoms and copper atoms in the crystal structure are exchanged. The final results show that the peak values of iron and copper in the anti-spinel are much higher than those of iron and copper in the spinel, so that the product is mainly of anti-spinel structure.

3.6 Elements Distribution

The elements distribution of product of A14211 is analyzed through Mapping (Fig.9).

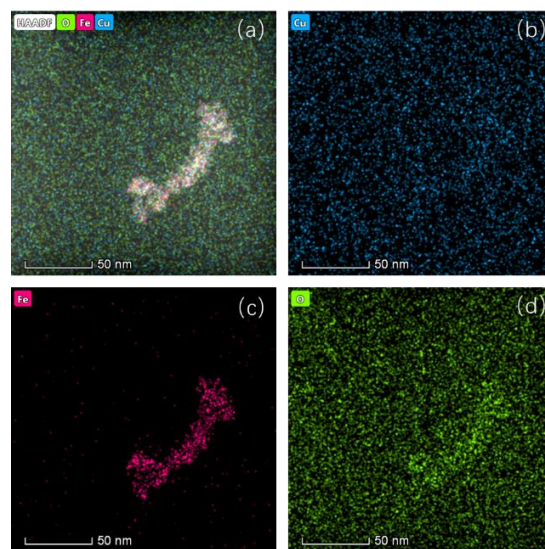


Fig.9 Mapping of A14211 Products. Distribution of total elements (a), copper (b), iron (c), oxygen (d) respectively

Iron is well concentrated on the product (Fig.9(c)), and copper distribution is difficult to distinguish (Fig.9(b)), because the solvent contains an amount of reduced copper. It may also be that the copper element is more than iron in the reaction process. The distribution of oxygen in products and solvents is different, but not obvious. The product is anti-spinel crystal, and the density of oxygen element is greater than that in solvent molecules.

4 Conclusion

In this article, a kind of ultra-small nano particle CuFe_2O_4 with uniform morphology was prepared by

solvothermal synthesis. The effects of different synthesis conditions on the size and morphology of nano particles were explored. XRD, TEM, EDS and other tests were used to characterize the materials, and the physical properties of the products were analyzed. The specific result is that the size of CuFe_2O_4 nanoparticles can be controlled by changing the ratio of synthetic raw materials, solvent and synthesis conditions; After optimizing the conditions, the characterization results showed that the materials synthesized at $280\text{ }^\circ\text{C}$ with triethylene glycol as solvent and PEG2000 as surfactant had high crystallinity and uniform morphology.

Acknowledgment

The experiments were done at Institute of Inorganic Nonmetallic Matter, HEU. The analysis supports were from Material Analysis and Testing Center, HEU. All costs of the experiments and tests are from the fund of Department of Material Science, HEU.

Reference

- [1] Peng, W., et al. (2020). *Journal of Dispersion Science and Technology* 41(14): 2211-2222.
- [2] He, F., et al. (2020). *Microchemical Journal* 158.
- [3] Singh, E., et al. (2021). *Materials Chemistry and Physics* 271.
- [4] Shaheen, W. M., et al. (2003). *Colloids and Surfaces a-Physicochemical and Engineering Aspects* 231(1-3): 51-65.
- [5] Ma, P. Y., et al. (2017). *Advanced Powder Technology* 28(11): 2797-2804.
- [6] El-Megharbel, S. M., et al. (2016). *Journal of Molecular Liquids* 216: 608-614.
- [7] Wang, J., et al. (2006). *Proceedings of the Royal Society a-Mathematical Physical and Engineering Sciences* 462(2069): 1355-1363.
- [8] Chen, J. Z., et al. (2014). *Crystal Research and Technology* 49(5): 309-314.
- [9] Chen, H. Q. and J. C. Ren (2012). *Analyst* 137(8): 1899-1903.
- [10] Watts, R. J., et al. (1999). *Journal of Hazardous Materials* 69(2): 229-243.
- [11] Klein, S., et al. (2021). *Acs Applied Bio Materials* 4(11): 7879-7892.
- [12] Wang, X. F., et al. (2015). *Chinese Journal of Catalysis* 36(12): 2211-2218.
- [13] Oda, Y., et al. (1998). *Japanese Journal of Applied Physics Part 1-Regular Papers Short Notes & Review Papers* 37(8): 4518-4521.
- [14] Jandl, S., et al. (2009). *Journal of Magnetism and Magnetic Materials* 321(21): 3607-3610.
- [15] Yang, X. L., et al. (2018). *Sensors and Actuators B-Chemical* 270: 538-544.
- [16] Dang, H. T. and T. K. Le (2016). *Journal of Sol-Gel Science and Technology* 80(1): 160-167.
- [17] Guo, R. (1991). *Acta Physico-Chimica Sinica* 7(6): 703-707.
- [18] Zhao, F. and J. K. Xu (2006). *Colloid and Polymer Science* 285(1): 113-117.
- [19] Sadiku-Agboola, O., et al. (2012). *Polish Journal of Chemical Technology* 14(1): 5-13.
- [20] Zhu, M. Y., et al. (2013). *Acs Applied Materials & Interfaces* 5(13): 6030-6037.
- [21] Huang, K., et al. (2012). *International Conference on Sustainable Energy and Environmental Engineering (ICSEEE 2012)*, Guangzhou, PEOPLES R CHINA.
- [22] Asnawi, S., et al. (2008). *International Conference on Nanoscience and Nanotechnology (NANO-SciTech 2008)*, Selangor, MALAYSIA.
- [23] Liu, R. M., et al. (2017). *Materials Research Express* 4(10).
- [24] Bohm, S. and O. Exner (2002). *Journal of Molecular Structure-Theochem* 578: 103-109.